Technical track: "SS19 Graphical Description for Modeling and Control of Power Systems"

Modeling of Automotive Control Systems Using Power Oriented Graphs

Riccardo Morselli, Roberto Zanasi
D.I.I. University of Modena and Reggio Emilia
Via Vignolese 905/b, Modena, 41100, Italy
E-mail: roberto.zanasi@unimore.it

***Abstract*— The basic idea of the Power-Oriented Graphs (POG) modeling technique is to use the power interaction between subsystems as basic concept for modeling. This approach is theoretically supported by the definition and the properties of the port-controlled Hamiltonian systems and allows the modeling of a wide variety of systems involving different energetic domains. Differently from the Bond Graphs technique, based on the same concept, the POG modeling technique solves explicitly the causality problem. By this way, the POG schemes are easily readable, close to the computer implementation and allow reliable simulations using every computer simulator. This paper introduces the properties of the POG technique and presents some examples related to automotive control systems.**

I. Introduction

Automotive control systems are often tested by hours of expensive tests and the final controls may be the result of a time consuming trial and error tuning. The availability of models that can be simulated on a computer can reduce the time and the costs required for the development of new control systems. This essentially happens for the following motivations:

- the models can be used in the early stage of a project as a design tool to determine the proper control laws and also to help the choice and the sizing of the system components;
- "hardware in the loop experiments" allow to test the correctness and the reliability of the ECU software without the need of road tests.

In order to make the development process based on models and simulations really valuable, the models must be reliable and, as far as possible, easily achievable. Moreover the models are usually shared among different people, therefore a common modeling language is needed to allow an easier and effective communication.

A modeling technique supported by physical properties together with a schematic representation based on some simple rules, would ease the writing of the models, would simplify the formal check of the models and would allow a common modeling language to share the models. This problem is in common between automotive control systems and many other research fields and a possible solution has been already proposed: the *bond graphs* modeling technique, see [1], [2] and the references therein. This modeling technique uses power interaction between systems as the basic concept for modeling. It has also a formal language to represent the basic components that may appear in a broad range of physical systems. However this technique has few drawbacks that makes it not completely suitable to satisfy the requirements cited above: the schematic representation needs more than 10 symbols and it is not easily readable; the "power" variables must be classified in "effort" and "flow" variables and finally the implementation of the bond graphs on a general purpose computer simulator may require a non trivial "translation" (causality problem).

As for *bond graphs*, the basic idea of the *Power-Oriented Graphs* (POG) modeling technique is to use the power interaction between subsystems as basic concept for modeling. Please refer to [3], [4] and [5] for further details. This approach is theoretically supported by the definition and the properties of the *Port-Controlled Hamiltonian systems* (PCH), see [6], and allows the modeling of a wide variety of systems involving different energetic domains. Differently from the bond graphs technique, the POG modeling technique uses only 3 basic symbols, does not need to classify the power variables and solves directly the causality problem. By this way, the POG schemes are easily readable, close to the computer implementation and allow reliable simulations using every computer simulator.

Several examples of application to real systems are available. Some of them, related to automotive control systems, are listed next and are validated by comparing the simulation results with experimental measurements. The POG technique is suitable to model systems involving different energetic domains. This is well shown in [12] where it is proposed a model for a "common rail" system that involves the electrical, hydraulic and mechanical domains. Similarly, the model presented in [13] has the same multi-domain feature. POGs have been applied to multi DOF robotic systems such as in [5] for a robot arm and in [10] for an head-neck model of a car passenger. Many examples can be finally found about vehicle systems and components: clutches and gearboxes in [14], [9], driveline in [8], limited slip differentials in [11] and in [15], semi-active suspensions in [17] and hydraulic hitch in [16].

The paper is organized as follows. Section II states the basic properties of the POG modeling technique. Section III shows the deep relations existing between the POG modeling technique and the *Port-Controlled Hamiltonian systems*. Finally, a valve and clutch models are described in Section IV to show a complex multi-domain application.

II. Power-Oriented Graphs: basic properties

The "Power-Oriented Graphs" are "signal flow graphs" combined with a particular "modular" structure essentially based on the two blocks shown in Fig. 1. The basic characteristic of this modular structure is the direct correspondence between pairs of system variables and real power flows: the product of the two variables involved in each dashed line of the graph has the physical meaning of "power flowing through the section". The two basic blocks shown in Fig. 1 are named

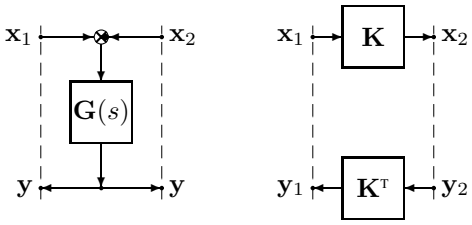

Fig. 1. Basic blocks: elaboration block (e.b.) and connection block (c.b.).

"elaboration block" (e.b.) and "connection block" (c.b.). The circle present in the e.b. is a summation element. When a black spot is present near to an entering arrow, the corresponding variable must be made negative before the sum operation. There is no restriction on $\mathbf{x}$ and $\mathbf{y}$ other than the fact that the inner product $\langle \mathbf{x}, \mathbf{y} \rangle = \mathbf{x}^{\mathrm{T}}\mathbf{y}$ must have the physical meaning of a "power".

The e.b. and the c.b. are suitable for representing both scalar and vectorial systems. In the vectorial case, $\mathbf{G}(s)$ and $\mathbf{K}$ are matrices: $\mathbf{G}(s)$ is always square, $\mathbf{K}$ can also be rectangular. While the elaboration block can store and dissipate energy (i.e. springs, masses and dampers), the connection block can only "transform" the energy, that is, transform the system variables from one type of energy-field to another (i.e. any type of gear reduction). In the linear vectorial case when $\mathbf{G}(s) = [\mathbf{M}\,s + \mathbf{R}]^{-1}$, ($\mathbf{M}$ is symmetric and positive definite) the energy E_s stored in the e.b. and the power P_d dissipating in the e.b. can be expressed as follows:

$$E_s = \frac{1}{2}\mathbf{y}^{\mathrm{T}}\mathbf{M}\,\mathbf{y}, \qquad P_d = \mathbf{y}^{\mathrm{T}}\mathbf{R}\,\mathbf{y}$$

There is a direct correspondence between POG representations and the corresponding state space descriptions. For example, the system

$$\left\{ \begin{array}{rcll} \mathbf{L}\,\dot{\mathbf{x}} & = & \mathbf{A}\mathbf{x} + \mathbf{B}\mathbf{u} & \qquad \mathbf{L} = \mathbf{L}^{\mathrm{T}} > 0 \\ \mathbf{y} & = & \mathbf{B}^{\mathrm{T}}\mathbf{x} & \end{array} \right. \qquad (1)$$

can be graphically represented with the POG shown in Fig. 2.

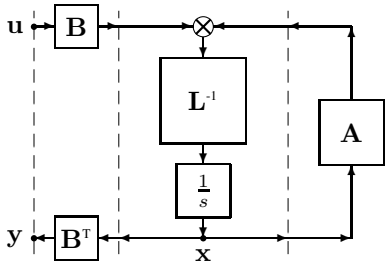

Fig. 2. Power oriented graph of a generic dynamic system.

When an eigenvalue of matrix $\mathbf{L}$ tends to zero (or to infinity), system (1) degenerates towards a lower dimension dynamic system. In this case, the dynamic model of the "reduced" system can be directly obtained from (1) by using a simple "congruent" transformation $\mathbf{x} = \mathbf{T}\mathbf{z}$ ($\mathbf{T}$ is constant):

$$\left\{ \begin{array}{c} \mathbf{T}^{\mathrm{T}}\mathbf{L}\mathbf{T}\dot{\mathbf{z}} = \mathbf{T}^{\mathrm{T}}\mathbf{A}\mathbf{T}\mathbf{z} + \mathbf{T}^{\mathrm{T}}\mathbf{B}\mathbf{u} \\ \mathbf{y} = \mathbf{B}^{\mathrm{T}}\mathbf{T}\mathbf{z} \end{array} \right. \Leftrightarrow \left\{ \begin{array}{c} \overline{\mathbf{L}}\dot{\mathbf{z}} = \overline{\mathbf{A}}\mathbf{z} + \overline{\mathbf{B}}\mathbf{u} \\ \mathbf{y} = \overline{\mathbf{B}}^{\mathrm{T}}\mathbf{z} \end{array} \right.$$

where $\overline{\mathbf{L}} = \mathbf{T}^{\mathrm{T}}\mathbf{L}\mathbf{T}$, $\overline{\mathbf{A}} = \mathbf{T}^{\mathrm{T}}\mathbf{A}\mathbf{T}$ and $\overline{\mathbf{B}} = \mathbf{T}^{\mathrm{T}}\mathbf{B}$. If matrix $\mathbf{T}$ is time-varying, an additional term $\mathbf{T}^{\mathrm{T}}\mathbf{L}\dot{\mathbf{T}}\mathbf{z}$ appears in the transformed system. When matrix $\mathbf{T}$ is rectangular, the system is transformed and reduced at the same time.

III. Power-Oriented Graph and port-controlled Hamiltonian systems

From a mathematical perspective, the *Port-Controlled Hamiltonian systems* (PCH) (see [6]) are natural candidates to model many real systems, as shown in the application examples cited in [7]. Basically, PCH are systems defined with respect to a geometric structure capturing the basic interconnection and dissipation laws with an *Hamiltonian* function given by the total stored energy of the system. A brief recall of some definitions given in [6] is given herein for reader convenience. The *Port-Controlled Hamiltonian system* (PCH) described in [6] are systems of the form:

$$\begin{array}{rcl} \dot{x} & = & [J(x) - R(x)]\,\dfrac{\partial H}{\partial x}(x) + g(x)u \\ y & = & g^T(x)\dfrac{\partial H}{\partial x}(x) \\ J(x) & = & -J^T(x) \\ R(x) & = & R^T(x) \geq 0 \end{array} \qquad (2)$$

One of the key feature of the PCH is the energy perspective in modeling the physical systems. The Hamiltonian $H(x)$ represents the energy stored in the system, the product $y^T\,u$ has the units of power and has the physical meaning of the power flowing through the port (u, y), indeed the power balance in (2) is:

$$y^T\,u = \frac{dH}{dt} + \frac{\partial H}{\partial x}^T R \frac{\partial H}{\partial x} \geq \frac{dH}{dt}$$

namely the power $y^T\,u$ supplied to the system is partially stored as energy and partially dissipated through R.

Many PCH can be obtained connecting different subsystems by power preserving interconnections. Let (u_1, y_1) and (u_2, y_2) be the power ports of two PCH, the general power preserving interconnection is the following:

$$\left[\begin{array}{c} u_1 \\ u_2 \end{array} \right] = \left[\begin{array}{cc} 0 & A \\ -A^T & 0 \end{array} \right] \left[\begin{array}{c} y_1 \\ y_2 \end{array} \right] \qquad (3)$$

where matrix A can also be time varying and/or state dependent. With the interconnection (3) the power flows from one system to the other without losses: $y_1^T\,u_1 = y_1^T\,A\,y_2 = y_2^T\,A^T\,y_1 = -y_2^T\,u_2$, namely the outcoming energy from one subsystem is exactly the incoming energy to the other.

To represent mechatronic systems as a set of PCH connected by power preserving interconnections, the definition (2) is not

enough, as shown in [17]. Some components of mechatronic systems may show a direct dissipation between the input u and the output y. A resistor is the simplest example. The PCH in (2) cannot describe such behaviour since the dissipation is only related to the gradient of $H(x)$. To describe mechatronic components that show direct dissipations, the following modification of (2) is proposed:

$$\begin{aligned} \dot{x} &= [J_1(x,v) - R_1(x,v)]\,\frac{\partial H}{\partial x}(x) + g(x,v)\,u \\ y &= g^T(x,v)\,\frac{\partial H}{\partial x}(x) + [R_2(x,v) - J_2(x,v)]\,u \\ & J_i(x,v) = -J_i^T(x,v) \qquad i=1,2 \\ & R_i(x,v) = R_i^T(x,v) \geq 0 \qquad i=1,2 \end{aligned} \tag{4}$$

where v is an external input vector that may also be equal to u. The matrix $J_2(x,v)$ models a direct change of the interconnection (example: ideal switch). The matrix $[J_2(x,v) - R_2(x,v)]$ has a similar meaning as the matrix D of the linear systems ($\dot{x} = A\,x + B\,u$, $y = C\,x + D\,u$).

The extended definition (4) preserves the basic properties of the PCHs and the energy perspective in modeling the physical systems. The inner product $y^T\,u$ has still the physical meaning of the power flowing through the port (u,y) and the power balance in (4) is the following:

$$\frac{dH}{dt} = y^T\,u - \frac{\partial H}{\partial x}^T\,R_1(x,v)\frac{\partial H}{\partial x} - u^T\,R_2(x,v)\,u \tag{5}$$

From (5) it is straightforward to verify that (4) satisfies the energy balance equation (EBE):

$$H(x(t)) - H(x(0)) = \int_0^t y^T(\tau)u(\tau)d\tau - D(t) \tag{6}$$

where $D(t)$ is a nonnegative function that captures the dissipation effects.

The relation between POG and PCH is straightforward. Let consider two interconnected PCH of the form (4) with state x_i, energy function $H_i(x_i)$, input u_i, output y_i and matrices $R_{i,1}$, $R_{i,2}$, $J_{i,1}$, $J_{i,2}$ and g_i (the state x_i and the input v_i have been suppressed to simplify the notation). The POG representation of the two interconnected PCH is shown in Fig. 3. Note that the interconnection is described by (3) but the minus sign is embedded in the second PCH to preserve the property that the interconnection preserves the power, indeed $y_1^T\,u_1 = -y_2^T\,u_2$. By this way the matrices g_i and A that have a very similar meaning have also the same representation.

The power flowing through the section ① of Fig. 3 is given by the inner product of the two variables of the power port:

$$P_1 = \frac{\partial H_1^T}{\partial x_1}\,R_{1,1}\,\frac{\partial H_1}{\partial x_1}$$

therefore P_1 is the (always positive) power dissipated by the dissipative elements described by $R_{1,1}$. Thanks to the minus sign in the sum node s_1, the power P_1 is dissipated from the (otherwise conservative) components described by the Hamiltonian $H_1(x_1)$. Similar considerations hold also for

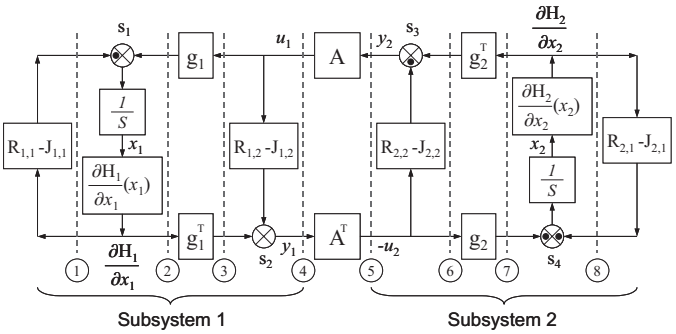

Fig. 3. Example of two interconnected PCH represented by POG.

the power port ⑧ of Fig. 3:

$$P_8 = \frac{\partial H_2^T}{\partial x_2}R_{2,1}\,\frac{\partial H_2}{\partial x_2}$$

The power P_2 and P_3 through the sections ② and ③ are always equal. Thanks to the plus sign on the right of the sum node s_1, the energy balance equation involving P_3 is:

$$\frac{dH_1}{dt} = \frac{\partial H_1^T}{\partial x_1}g_1\,u_1 - \frac{\partial H_1^T}{\partial x_1}R_{1,1}\frac{\partial H_1}{\partial x_1} = P_3 - \frac{\partial H_1^T}{\partial x_1}R_{1,1}\frac{\partial H_1}{\partial x_1}$$

that is the energy balance equation of a PCH in the form (2).

Also the powers P_6 and P_7 are equal, due to the minus sign on the left of the sum node s_4, the energy balance equation involving P_6 takes the form:

$$\frac{dH_2}{dt} = \frac{\partial H_2^T}{\partial x_2}g_2\,u_2 - \frac{\partial H_2^T}{\partial x_2}R_{2,1}\frac{\partial H_2}{\partial x_2} = -P_6 - \frac{\partial H_2^T}{\partial x_2}R_{2,1}\frac{\partial H_2}{\partial x_2}$$

Finally the powers P_4 and P_5 through the sections ④ and ⑤ are always equal. Let $P_A = P_4 = P_5$, by noting that:

$$\begin{aligned} P_2 = P_3 &= P_A - u_1^T\,R_{1,2}\,u_1 \\ P_7 = P_6 &= -P_A - u_2^T\,R_{2,2}\,u_2 \end{aligned}$$

the energy balance equation for the system shown in Fig. 3 is:

$$\begin{aligned} \frac{dH_1}{dt} &= P_A - u_1^T\,R_{1,2}\,u_1 - P_1 \\ \frac{dH_2}{dt} &= -P_A - u_2^T\,R_{2,2}\,u_2 - P_8 \end{aligned}$$

then if $P_A > 0$ the power P_A is flowing from subsystem 2 to subsystem 1.

To give an example let consider the two linear electric circuits shown in Fig. 4. The PCH equations of the RLR circuit are the following:

$$\begin{aligned} \dot{\varphi} &= [-r_{1,1}]\,\frac{\partial H_1}{\partial \varphi} + [1 \quad -1]\begin{bmatrix} V_{i1} \\ V_{i2} \end{bmatrix} \\ \begin{bmatrix} I_{o1} \\ I_{o2} \end{bmatrix} &= \begin{bmatrix} 1 \\ -1 \end{bmatrix}\frac{\partial H_1}{\partial \varphi} + \begin{bmatrix} 1/r_{1,2} & -1/r_{1,2} \\ -1/r_{1,2} & 1/r_{1,2} \end{bmatrix}\begin{bmatrix} V_{i1} \\ V_{i2} \end{bmatrix} \\ H_1 &= \frac{1}{2}\frac{\varphi^2}{L} \;\Rightarrow\; \frac{\partial H_1}{\partial \varphi} = \frac{\varphi}{L} = I_L \end{aligned} \tag{7}$$

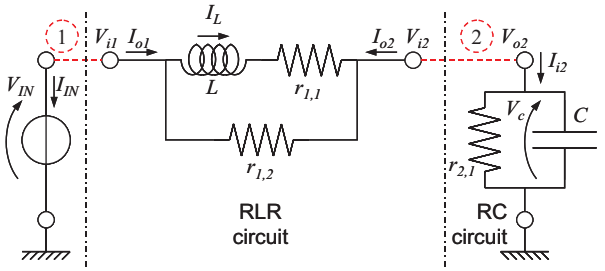

Fig. 4. Example of three connected electric circuits.

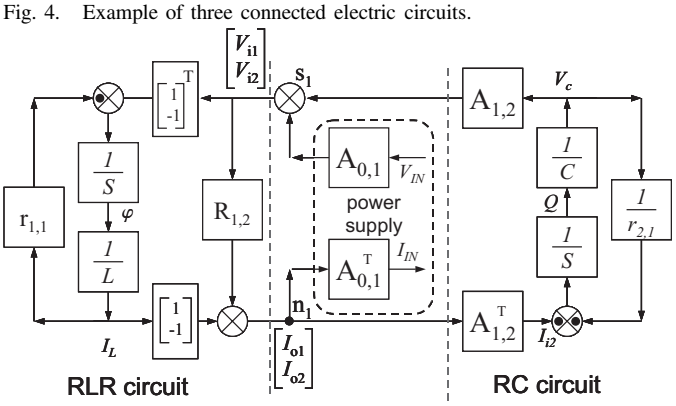

Fig. 5. Example of POG corresponding to the three connected electric circuits shown in Fig. 4.

The direct dissipation term is due to the resistor $r_{1,2}$ and the matrix $R_{1,2}$ corresponding to equation (5) is given by:

$$R_{1,2} = \begin{bmatrix} 1/r_{1,2} & -1/r_{1,2} \\ -1/r_{1,2} & 1/r_{1,2} \end{bmatrix} = \begin{bmatrix} 1 \\ -1 \end{bmatrix} \begin{bmatrix} \dfrac{1}{r_{1,2}} \end{bmatrix} \begin{bmatrix} 1 & -1 \end{bmatrix}$$

The PCH equations of the RC circuit are the following:

$$\begin{aligned} \dot{Q} &= \left[-\frac{1}{r_{2,1}} \right] \frac{\partial H_2}{\partial Q} + I_{i,2} \\ V_{o2} &= \frac{\partial H_2}{\partial Q} = V_c \\ H_2 &= \frac{1}{2}\frac{Q^2}{C} \quad \Rightarrow \quad \frac{\partial H_2}{\partial Q} = \frac{Q}{C} = V_c \end{aligned} \tag{8}$$

The power preserving connection between the RLR circuit and the power supply (corresponding to the dashed line (1) shown in Fig. 4) is obtained by the following equation:

$$\begin{bmatrix} V_{i1} \\ V_{i2} \\ I_{IN} \end{bmatrix} = \begin{bmatrix} 0 & 0 & 1 \\ 0 & 0 & 0 \\ -1 & 0 & 0 \end{bmatrix} \begin{bmatrix} I_{o1} \\ I_{o2} \\ V_{IN} \end{bmatrix} \tag{9}$$

The power preserving connection between the RLR circuit and the RC circuit (corresponding to the dashed line (2) shown in Fig. 4) is obtained by the following equation:

$$\begin{bmatrix} V_{i1} \\ V_{i2} \\ I_{i2} \end{bmatrix} = \begin{bmatrix} 0 & 0 & 0 \\ 0 & 0 & 1 \\ 0 & -1 & 0 \end{bmatrix} \begin{bmatrix} I_{o1} \\ I_{o2} \\ V_{o2} \end{bmatrix} \tag{10}$$

The two equations (9) and (10) have the same form as (3) with $A = [1 \;\; 0]^T = A_{0,1}$ and $A = [0 \;\; 1]^T = A_{1,2}$ respectively. The POG corresponding to Fig. 4 and equations (7), (8), (9) and (10) is shown in Fig. 5. This POG follows the basic rules stated

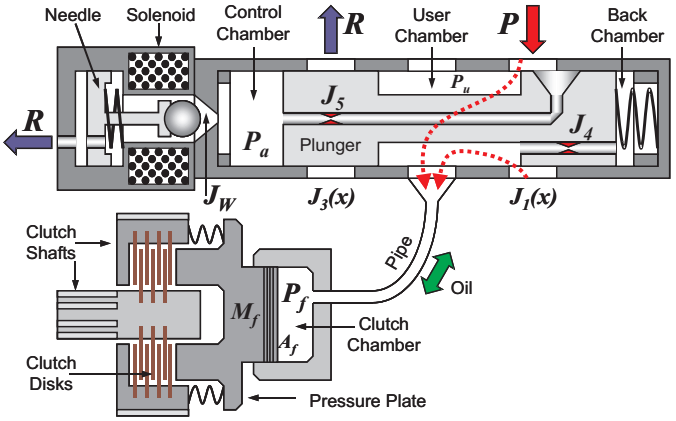

Fig. 6. Clutch control system: control valve (enlarged and partially connected to the hydraulic power supply P) and wet-clutch schematic representation.

before, unfortunately to represent POGs on a flat paper may happen that some subsystems "overlap" (i.e. the RC and the power supply POGs). The connection among the subsystems is power preserving if for each node corresponds a sum node on the conjugate power variable (i.e. the node n_1 and the sum node s_1 of Fig. 5):

$$y_1^T u_1 = y_1^T (u_2 + u_3) = y_1^T u_2 + y_1^T u_3$$

IV. Application Example: Electro-Hydraulic Clutch Actuator

Multi-plate wet clutches are often used in many automotive applications where high torques, high resistance and high durability are required. Common applications include automatic transmission gearboxes and limited slip differentials. Modern electronic controls operate the clutch by an hydraulic actuator and an electro-valve. The torque transmitted through the shafts depends mainly on the clutch-actuator internal oil pressure and this pressure is controlled by means of the electro-valve. A simplified scheme of a such system is shown in Fig. 6. For further details please refer to [13]. This system can be divided into four interacting subsystems: the valve plunger, the control chamber, the user chamber and the actuator.

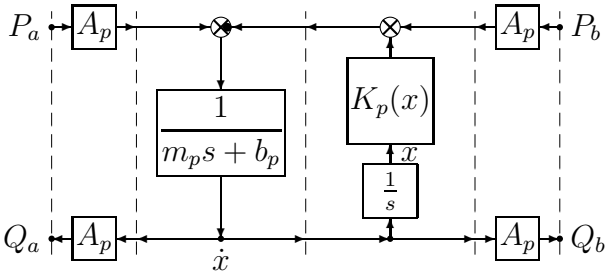

Fig. 7. Valve plunger subsystem POG model

The valve plunger subsystem POG model is shown in Fig. 7. Let x and $\dot{x}$ denote, respectively, the plunger position and velocity. The plunger mass m_p moves subject to the forces coming from the viscous friction coefficient b_p, the return spring $K_p(x)$ and the pressures P_a and P_b of the control

chamber and of the back chamber, respectively. The nonlinear force $K_p(x)$ models both the force of the return spring and the contact force between the plunger and the plunger case at the two extreme plunger positions. The plunger motion causes the oil flows Q_a and Q_b through the control chamber and the back chamber, respectively.

$$\begin{aligned} m_p\ddot{x} &= (P_a - P_b)A_p - b_p\dot{x} - K_p(x) \\ Q_a &= Q_b = A_p\dot{x} \end{aligned} \tag{11}$$

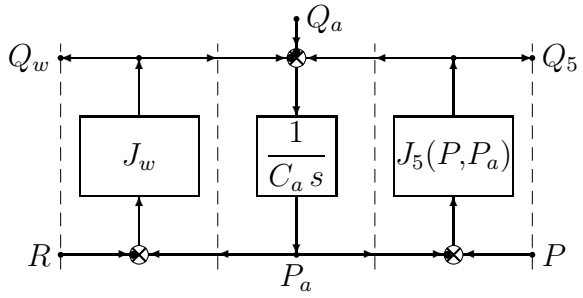

Fig. 8. Control chamber POG model

The pressure P_a in the control chamber is determined by the integration of three oil flows in the hydraulic capacity C_a: the oil flow Q_5 coming from the hydraulic power supply P, the flow Q_a due to the plunger motion and the flow Q_w through the variable discharge orifice. The very small hydraulic capacity C_a stores potential energy in terms of oil pressure and it takes into account the small elastic deformation of the valve case and the high oil stiffness:

$$C_a\dot{P}_a = Q_5 - Q_a - Q_w \tag{12}$$

The flows Q_5 and Q_w are nonlinear functions of the pressures P, P_a and R:

$$\begin{aligned} Q_5 &= C_{d5}\sqrt{|P - P_a|}\,\mathrm{sgn}(P - P_a) = J_5(P, P_a) \\ Q_w &= C_{dw}(I)\sqrt{|P_a - R|}\,\mathrm{sgn}(P_a - R) = J_w(I, P_a, R) \end{aligned} \tag{13}$$

The discharge coefficient C_{dw} can be varied by the control current I. In the real system C_{dw} is function of the sphere position which is determined by the pressure P_a and by the needle force due to the current I. Experimental measurements showed that the discharge coefficient C_{dw} can be approximated as a nonlinear function of the control current $C_{dw} = C_{dw}(I)$ with negligible errors. Equations (12) and (13) lead to the POG model shown in Fig. 8.

Depending on the plunger position x, the output user chamber is connected either to the power supply P through the variable orifice J_1 or to the oil tank by the orifice J_3, see eq. (14). The user chamber is connected to the back chamber through orifice J_4. This orifice plays two fundamental roles: it implements the feedback action since P_b becomes a "measure" of the user pressure P_u, and it has damping effect that avoids plunger oscillations.

$$\begin{aligned} Q_1 &= C_{d1}(x)\sqrt{|P - P_u|}\,\mathrm{sgn}(P - P_u) = J_1(x, P, P_u) \\ Q_3 &= C_{d3}(x)\sqrt{|P_u - R|}\,\mathrm{sgn}(P_u - R) = J_3(x, P_u, R) \\ Q_4 &= C_{d4}\sqrt{|P_b - P_u|}\,\mathrm{sgn}(P_b - P_u) = J_4(P_b, P_u) \end{aligned} \tag{14}$$

The back chamber and the user chamber are modeled as two small hydraulic capacities as for the control chamber:

$$\begin{aligned} C_b\dot{P}_b &= Q_b - Q_4 \\ C_u\dot{P}_u &= Q_1 + Q_4 - Q_3 - Q_u \end{aligned} \tag{15}$$

Equations (14) and (15) are graphically represented by the POG dynamic model of Fig. 9

A pipe connects the valve user chamber to the clutch chamber. The dynamic effects of this pipe cannot be neglected and they are described by four elements: the user chamber capacity C_u, the hydraulic resistance R_f, the pipe hydraulic inductance L_f and the clutch chamber capacity C_f:

$$\begin{aligned} L_f\dot{Q}_u &= P_l - P_f = P_u - P_{Q_u} - P_f \\ P_u - P_l &= \frac{Q_u\,|Q_u|}{C_{df}} = R_f(Q_u) \\ C_f\dot{P}_f &= Q_u - A_f\,\dot{z} \end{aligned} \tag{16}$$

Equations (16) defines the left part of the POG model of Fig. 10. The right part represents the motion of the pressure plate under the effects of the pressure P_f, the elastic force $K_M(z)$ and the viscous friction b_f:

$$\begin{aligned} m_f\ddot{z} &= P_f A_f - b_f\dot{z} - K_M(z) - K_{bc}\,\mathrm{sgn}(\dot{z}) \\ K_M(z) &= K_F(z) + K_D(z) \end{aligned} \tag{17}$$

The elastic force $K_M(z)$ is the sum of two contribution: $K_F(z)$ represents the force of the return springs and the contact with the gearbox at the two extreme pressure plate positions; $K_D(z)$ is the force generated by the compression of the clutch discs that determines the maximum torque through the clutch.

The result of a measure with a two step input current compared with the corresponding simulation is shown in Fig. 11. Due to a non disclosure agreement the figure axes are normalized. The simulations are very similar to the experimental data proving that the modeling approach is suitable to this kind of multi-domain systems.

V. Conclusion

The paper has described the *Power-Oriented Graphs* (POG) modeling technique. This modeling technique is supported by physical properties and has a schematic representation based on few simple rules and symbols that makes it easily readable and close to the implementation on computer simulators. Thanks to its properties, the POG modeling technique is a natural candidate to model a broad range of multi-domain (automotive) control systems and to define a common modeling language.

References

[1] Paynter, H.M., *Analysis and Design of Engineering Systems*, MIT-press, Camb., MA, 1961.

[2] D. C. Karnopp, D.L. Margolis, R. C. Rosemberg, *System dynamics - Modeling and Simulation of Mechatronic Systems*, Wiley Interscience, ISBN 0-471-33301-8, 3rd ed. 2000.

[3] R. Zanasi, "Power Oriented Modelling of Dynamical System for Simulation", *IMACS Symp. on Modelling and Control of Technological System*, Lille, France, May 1991.

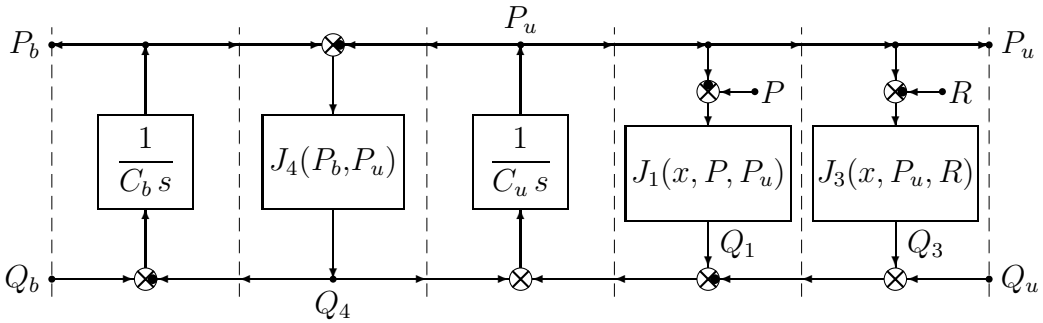

Fig. 9. Back chamber and output user chamber POG models

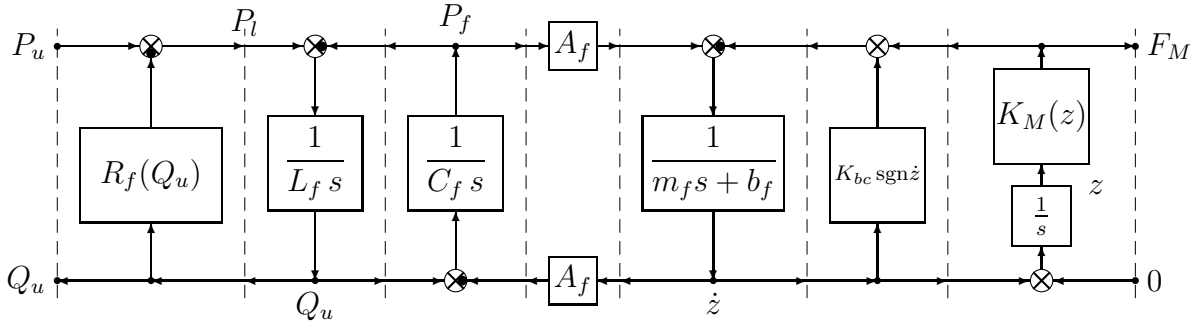

Fig. 10. Clutch actuator POG model

[4] R. Zanasi, K. Salisbury, "Dynamic Modeling, Simulation and Parameter Identification for the WAM Arm", *A.I. Memo No. 1387*, MIT, Cambridge, USA, August 1992.

[5] Zanasi R., "Dynamics of a n-links Manipulator by Using Power-Oriented Graph", *SYROCO '94*, Capri, Italy, 1994.

[6] A.J. van der Schaft, *L2-Gain and Passivity Techniques in Nonlinear Control*, Springer Communications and Control Engineering series, 2nd ed., Springer-Verlag, ISBN 1-85233-073-2, 2000.

[7] R. Ortega, A. van der Schaft, B.M. Maschke, G. Escobar, "Interconnection and damping assigment passivity-based control of port-controlled Hamiltonian systems", *Automatica*, Vol. 38, p:585-596, 2002.

[8] R. Zanasi , A. Visconti, G. Sandoni, R. Morselli, "Dynamic Modeling and Control of a Car Transmission System", *International Conference on Advanced Intelligent Mechatronics*, Como, Italy, July 8-12, 2001.

[9] R. Zanasi, G. Sandoni, R. Morselli, "Simulation of a Variable Dynamic Dimension Systems: the clutch example", *European Control Conference (ECC'01)*, Porto (Portugal), September, 2001.

[10] R. Zanasi, R. Morselli, A. Visconti, M.Cavanna, "Head-neck Model for the Evaluation of Passenger's Comfort ". *Proc. of the Intl. Conference on Intelligent Robots and Systems - IROS'02*, Lausanne, Switzerland, 2002.

[11] R. Zanasi, G. Sandoni, R. Morselli, "Mechanical and Active Car Differential: Detailed and Reduced Dynamic Models", *proceedings of the Symposium on Mathematical Modelling - MATHMOD'03*, Vien, Austria, pp. 1011-1020, ISBN:3-901608-24-9, February 2003.

[12] R. Morselli, E. Corti, G. Rizzoni, "Energy Based Model of a Common Rail Injector", *Conference on Control Applications (CCA'02)*, Glasgow, Scotland, September 18-20, 2002.

[13] R. Morselli, R. Zanasi, R. Cirsone, E. Sereni, E. Bedogni, E. Sedoni, "Dynamic Modeling and Control of Electro-Hydraulic Wet Clutches". *Proc. of the* 6^{th} *International Conference on Intelligent Transportation Systems - ITSC'03*, Shanghai, China, October, 12-15, 2003.

[14] R. Morselli, R. Zanasi, P. Ferracin, "Modeling and Simulation od Static and Coulomb Friction in a Class of Automotive Systems". *International Journal of Control*, Vol.79, No.5, May 2006, pp.508-520.

[15] R. Morselli, R. Zanasi, G. Sandoni, "Detailed and Reduced Dynamic Models of Passive and Active Limited-slip Car Differentials". *Mathematical and Computer Modeling of Dynamical Systems*, Vol.12, No.4, August 2006, pp.347-362.

[16] R. Morselli, R. Zanasi, P. Ferracin, "Dynamic Model of an Electro-Hydraulic Three Point Hitch", *Proc. of the American Control Conference - ACC'06*, Minneapolis, Minnesota, USA, June 14-16, 2006.

[17] R. Morselli, R. Zanasi, "Control of Mechatronic Systems by Dissipative Devices: Application to Semi-Active Vehicle Suspensions", *Proc. of the American Control Conference - ACC'06*, Minneapolis, Minnesota, USA, June 14-16, 2006.

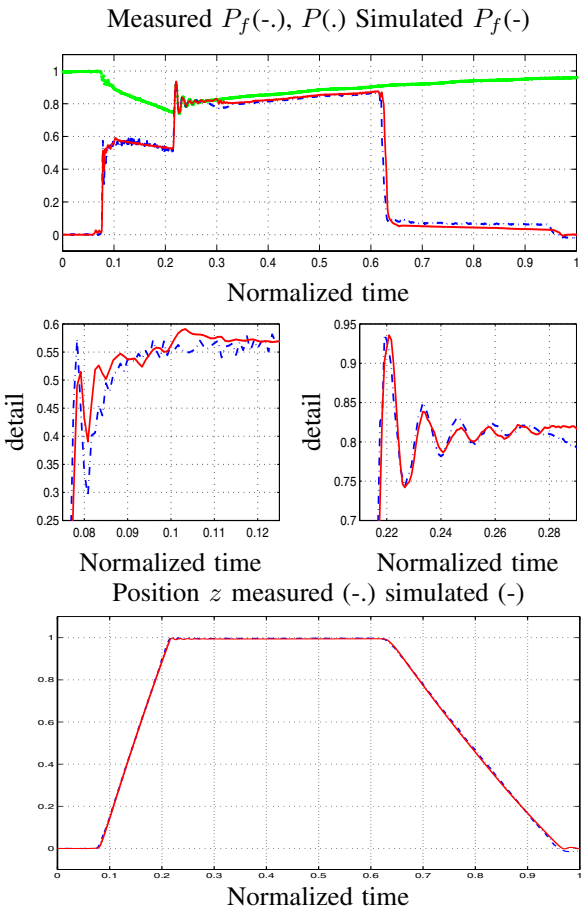

Fig. 11. Step input measurements. Left: supply pressure P (dotted), clutch chamber pressureP_f measured (dash-dotted) and simulated (solid). Right: Clutch actuator position z: measured (dash-dotted) and simulated (solid).